

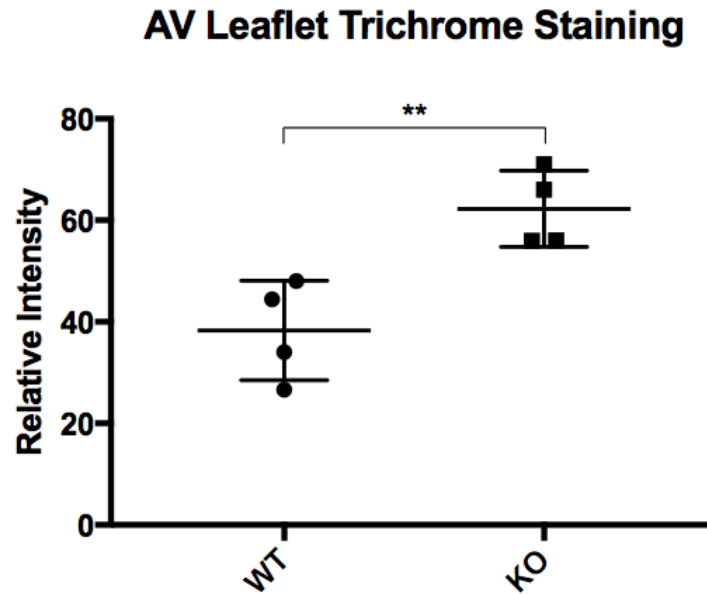
Supplemental Material

Table S1. De-identified patient details are provided for the human tissue western blot.

| Lane | Sample (Loading Amount) | Publication ID | Age | Gender | Race | Failing Category | Cause of Death | Ejection Fraction | Left Ventricular Assist Device |
|------|-------------------------|----------------|-----|--------|-----------|---|---|--------------------------------|--------------------------------|
| 4 | Myocardium (2.5µg) | 947200 | 63 | Female | Caucasian | Non-failing | Motor vehicle accident; Head trauma | Echocardiography not performed | No |
| 5 | AV (10µg) | 147381 | 58 | Male | Caucasian | Non-failing | Blunt injury; Subdural hemorrhage | 65% | No |
| 6 | AV (10µg) | 219852 | 30 | Female | Caucasian | Non-failing | Unknown cause of death; Sudden cerebral edema and respiratory failure | 55% | No |
| 7 | AV (10µg) | 364587 | 19 | Male | Caucasian | Non-failing | Blunt injury; Motor vehicle accident | 25% | No |
| 8 | AV (10µg) | 712301 | 67 | Male | Caucasian | Non-failing | Blunt injury; Intraparenchymal hemorrhage | Echocardiography not performed | No |
| 9 | AV (10µg) | 947200 | 63 | Female | Caucasian | Non-failing | Motor vehicle accident; Head trauma | Echocardiography not performed | No |
| 10 | AV (10µg) | 328163 | 63 | Male | Caucasian | Failing; Ischemic heart disease; Moderate to severe aortic stenosis | N/A | 15-20% | No |

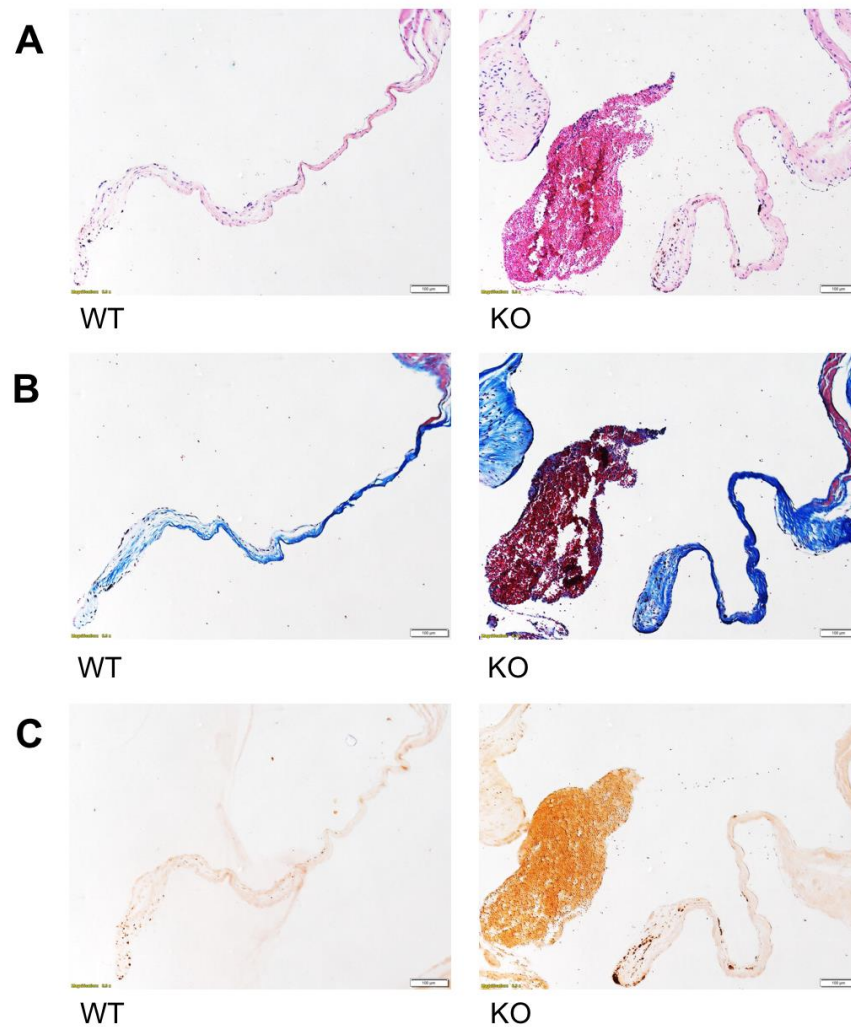
Healthy aortic valves were excised from non-failing hearts from donors who had been declared deceased from non-cardiac conditions as noted in the “Cause of Death” column. The stenotic aortic valve was excised from a failing heart from a patient undergoing cardiac transplantation. No aortic valves were from patients with left ventricular assist devices were used, ensuring the all valves experienced physiological, pulsatile blood flow. AV, aortic valve.

Figure S1. Intensity of the trichrome staining in mouse aortic valve.



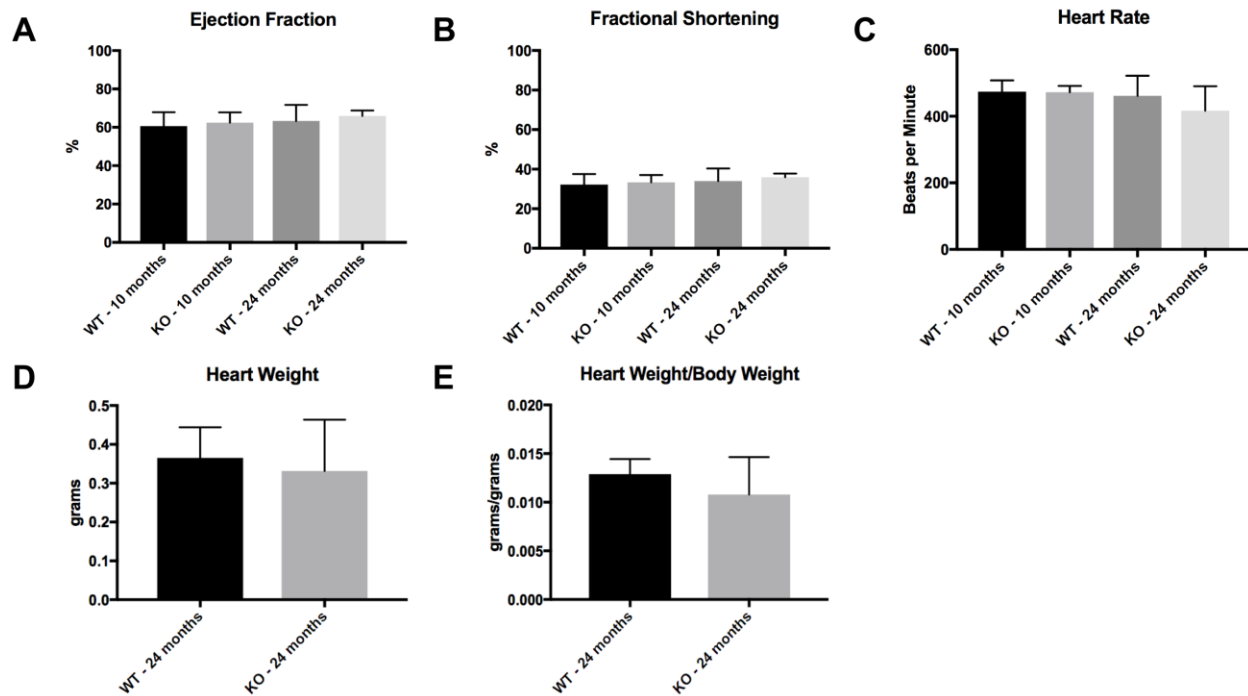
Intensity of trichrome staining in the mouse aortic valve (data presented in Figure 2D) was calculated. Significant difference was observed between the wild type and *Mg53*^{-/-} mice. A two-tailed Student's t-test was used to obtain the p-value. **p<0.01

Figure S2. Coronal sections of mitral valve leaflets are shown opening downwards, left ventricle below and left atrium above.



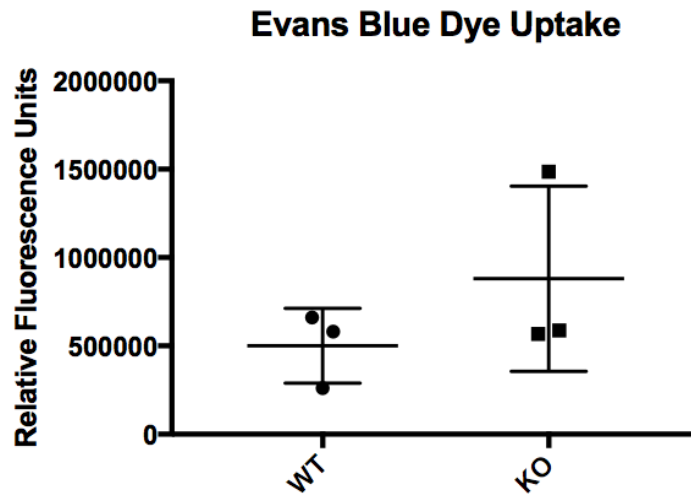
Mitral valve leaflets (n=2) of aged wild type (left) and *Mg53*^{-/-} (right) mice showed similar trends as aortic valves in leaflet (A) thickness (via H&E), (B) fibrosis (via Masson's trichrome), and (C) calcification (via Alizarin Red S). WT, wild type; KO, knockout (*Mg53*^{-/-}).

Figure S3. Wild type and *Mg53*^{-/-} mice show similar cardiac function.



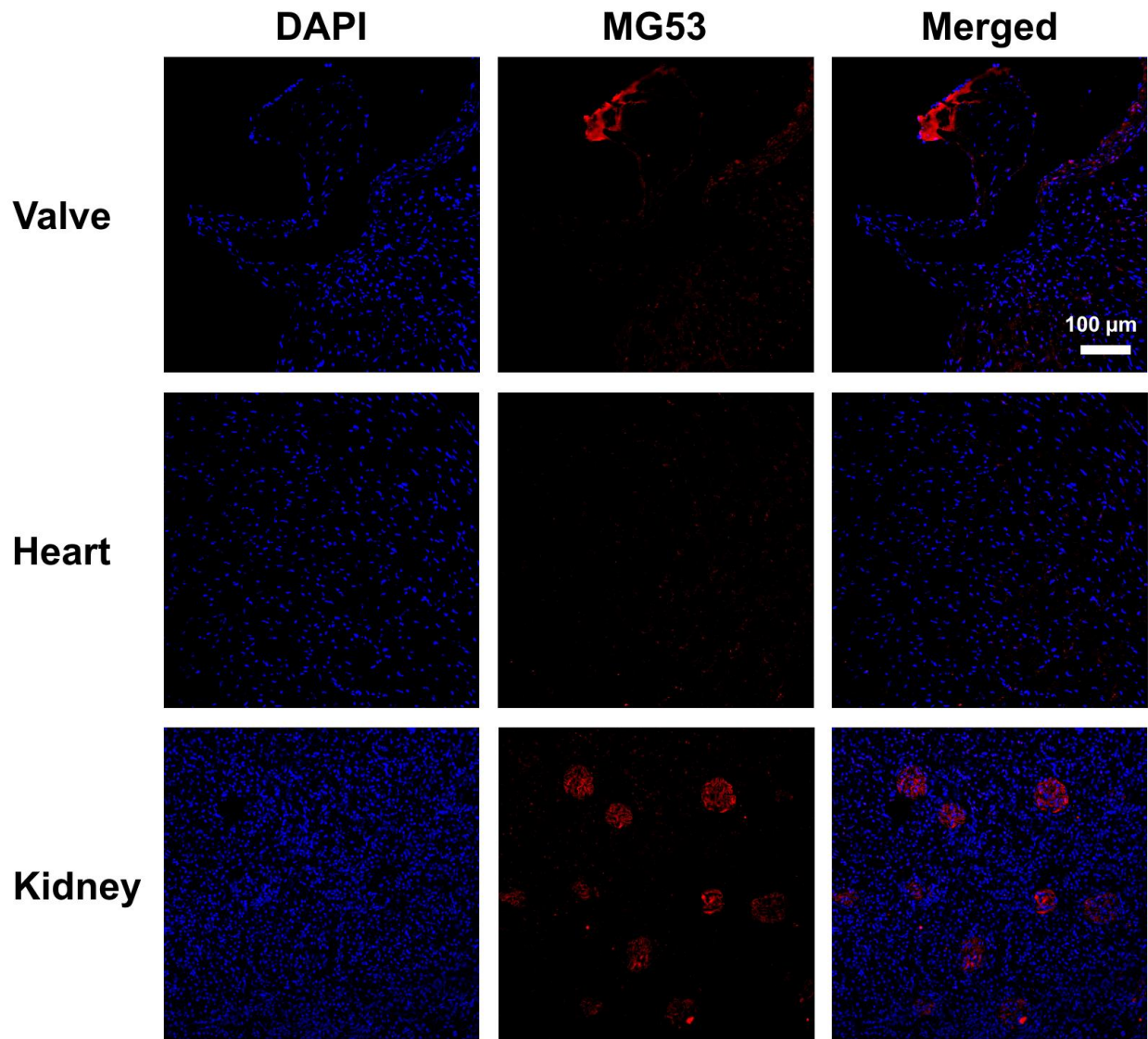
No statistical differences in left ventricular ejection fraction (EF) (A), fractional shortening (FS) (B), heart rate (HR) (C), heart weight (D), and ratio of heart weight/body weight (E) were noted between wild type and *Mg53*^{-/-} mice. EF and FS measurements were made with mice in reverse Trendelenburg position. Ages of the mouse groups are listed. Significance was tested via two-way ANOVA tests with Tukey's multiple comparison testing ($\alpha=0.05$, Figures S3A-S3C) and two-tailed Student's t-tests (Figures S3D-S3E), showing no statistically significant differences between groups. WT, wild type; KO, knockout (*Mg53*^{-/-}).

Figure S4. Evans blue dye (EBD) uptake in a limited number of younger wild type and *Mg53*^{-/-} littermate mice.



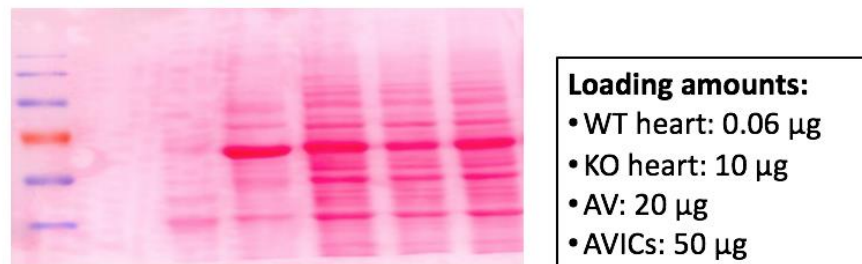
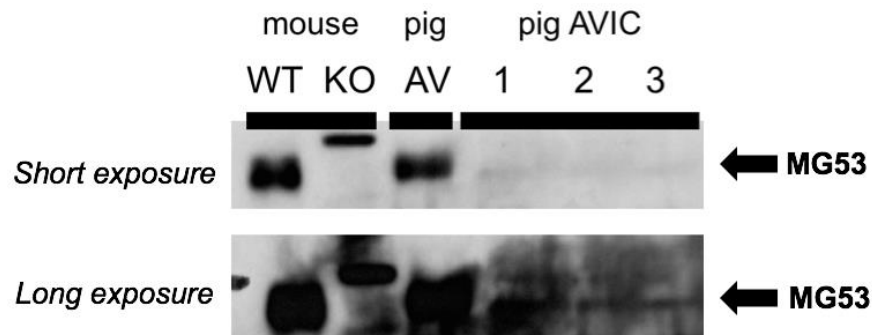
2 pairs are 7 months and 1 pair is 17 months age. EBD was administered to littermate wild type and *Mg53*^{-/-} mice via intraperitoneal injection. Mice were euthanized 24 hours post-injection, and hearts were excised and OCT-embedded for cryosectioning. Histological examination was used to locate the aortic valve, and the intensity of EBD uptake was quantified with no statistically significant difference observed.

Figure S5. Systemically administered rhMG53 protein can penetrate murine aortic valve tissue.



Mg53^{-/-} mouse (24 months age) was intravenously injected with 2 mg/kg rhMG53 for 4 hours. Afterwards, the heart was excised, cryo-embedded, and stained for MG53. We observed uptake of rhMG53 in the aortic valve leaflet (red, top row) but not in the myocardium of the *Mg53*^{-/-} mouse (middle row). As rhMG53 is excreted via the kidney, we also observe rhMG53 uptake in the renal glomeruli (bottom row). DAPI was used to stain the cell nuclei.

Figure S6. Western blot of MG53 expression in the pig aortic valvular interstitial cells (AVICs).



While short exposure did not reveal the presence of the 53 kDa band in the western blot (top), longer exposures showed that native MG53 (53 kDa, arrow) is expressed in pig AVICs. Wild type mouse myocardium (0.06 µg) and pig aortic valve tissue (20 µg) were used as positive controls and *Mg53*^{-/-} myocardium (10 µg) as a negative control. 50 µg of lysates from pig AVICs were loaded from three different animals (1, 2, 3).

Supplemental Video Legends

Videos S1-S2. Representative color Doppler videos from 24-month-old wild type (left) and *Mg53*^{-/-} (right) mice. Best viewed with Windows Media Player.

Video S3. GFP-MG53 translocates to VIC membrane injury site after microelectrode needle penetration. Best viewed with Windows Media Player.